© 2017. Published by The Company of Biologists Ltd | Development (2017) 144, 1242-1248 doi:10.1242/dev.141598

RESEARCH REPORT

Phosphorylation potential of *Drosophila* E-Cadherin intracellular domain is essential for development and adherens junction biosynthetic dynamics regulation

Yi-Jiun Chen[1], Juan Huang[1,2], Lynn Huang[1], Erin Austin[1] and Yang Hong[1,*]

ABSTRACT

Phosphorylation of a highly conserved serine cluster in the intracellular domain of E-Cadherin is essential for binding to β-Catenin *in vitro*. In cultured cells, phosphorylation of specific serine residues within the cluster is also required for regulation of adherens junction (AJ) stability and dynamics. However, much less is known about how such phosphorylation of E-Cadherin regulates AJ formation and dynamics *in vivo*. In this report, we generated an extensive array of *Drosophila* E-Cadherin (DE-Cad) endogenous knock-in alleles that carry mutations targeting this highly conserved serine cluster. Analyses of these mutations suggest that the overall phosphorylation potential, rather than the potential site-specific phosphorylation, of the serine cluster enhances the recruitment of β-Catenin by DE-Cad *in vivo*. Moreover, phosphorylation potential of the serine cluster only moderately increases the level of β-Catenin in AJs and is in fact dispensable for AJ formation *in vivo*. Nonetheless, phosphorylation-dependent recruitment of β-Catenin is essential for development, probably by enhancing the interactions between DE-Cad and α-Catenin. In addition, several phospho-mutations dramatically reduced the biosynthetic turnover rate of DE-Cad during apical-basal polarization, and such biosynthetically stable DE-Cad mutants specifically rescued the polarity defects in embryonic epithelia lacking the polarity proteins Stardust and Crumbs.

KEY WORDS: DE-Cadherin, β-Catenin, Shotgun, Armadillo, α-Catenin, Adherens junctions, Apical-basal polarity, *Drosophila*, Crb, Sdt

INTRODUCTION

Adherens junction (AJ) complexes are composed of the transmembrane protein E-Cadherin and cytosolic proteins β-Catenin (β-Cat) and α-Catenin (α-Cat) (Harris and Tepass, 2010). Direct binding between β-Catenin and the intracellular tail of E-Cadherin is essential for AJ complex formation and trafficking. Such interaction also recruits α-Catenin, which links the AJ complex to the F-actin network (Buckley et al., 2014). Previous studies have identified a highly conserved serine cluster in the E-Cadherin intracellular tail phosphorylation of which drastically increases the binding affinity of E-Cadherin to β-Catenin by ∼800 fold *in vitro* (Choi et al., 2006; Huber and Weis, 2001; Lickert et al., 2000). In addition, cell culture studies showed that phosphorylation of specific serine residues within the cluster could play distinct roles in regulating AJ formation and stability (Choi et al., 2015; Lickert et al., 2000; McEwen et al., 2014). In *Drosophila*, we previously reported that the biosynthetic turnover of AJs is differentially regulated during apical-basal polarization in *Drosophila* embryonic epithelia (Huang et al., 2011). The increased AJ stability in polarized cells coincides with the stronger binding between *Drosophila* E-Cadherin (DE-Cad, also known as Shotgun or Shg) and β-Catenin (also known as Armadillo or Arm; Peifer and Wleschaus, 1990) (Huang et al., 2011), making DE-Cad phosphorylation an attractive mechanism for modulating the DE-Cad/β-Catenin interaction during cell polarization.

Nonetheless, it remains to be determined whether phosphorylation of the conserved serine cluster in E-Cadherin plays significant roles in AJ formation, development and cell polarity *in vivo*. Recent studies in *Caenorhabditis elegans* based on transgenic expression of phospho-mutant E-Cadherins suggest a requirement of site-specific phosphorylation in the serine cluster for development, but it is unknown how β-Catenin binding is affected *in vivo* in such mutants (Choi et al., 2015). Using our genomic engineering method (Huang et al., 2009), we generated an extensive array of *Drosophila DE-cadherin* knock-in alleles carrying specific deletions and phospho-mutations in the conserved serine cluster. One unique advantage of these knock-in mutants is that all mutant DE-Cad proteins are expressed from the endogenous locus to allow clean and consistent genetic assays. Using such engineered *DE-Cad* knock-in alleles exclusively, we first aimed to confirm whether the conserved serine cluster is essential for function of DE-Cad in AJ formation and development. Second, we aimed to determine how the phosphorylation potential of the serine cluster is required for DE-Cad to interact with β-Catenin and α-Catenin *in vivo*. Finally, we also aimed to identify potential site-specific phosphorylations that might interact with the apical polarity complex Stardust (Sdt)-Crumbs (Crb) to regulate the AJ formation and dynamics during apical-basal polarization.

RESULTS AND DISCUSSION

A short motif containing the conserved serine cluster in the DE-Cad intracellular domain is essential for AJ formation *in vivo*

The intracellular tail of E-Cadherin contains two functional domains: a juxtamembrane domain that regulates steady-state levels of the AJ complex by interacting with p120-catenin (Adherens junction protein p120, p120ctn), and a C-terminal motif that is required for binding β-Catenin (Fig. 1A,B) (Nagafuchi et al., 1994; Oda et al., 1993; Pacquelet et al., 2003; Stappert and Kemler, 1994). To narrow down further the minimal motif in

[1]Department of Cell Biology, University of Pittsburgh Medical School, Pittsburgh, PA 15261, USA. [2]Department of Biotechnology, School of Basic Medical Sciences, Nanjing Medical University, Nanjing 211166, People's Republic of China.

*Author for correspondence (yhong@pitt.edu)

J.H., 0000-0002-6259-4196; E.A., 0000-0001-9379-3457; Y.H., 0000-0003-2252-0798

Received 28 June 2016; Accepted 7 February 2017

Development (2017) 144, 1242-1248 doi:10.1242/dev.141598

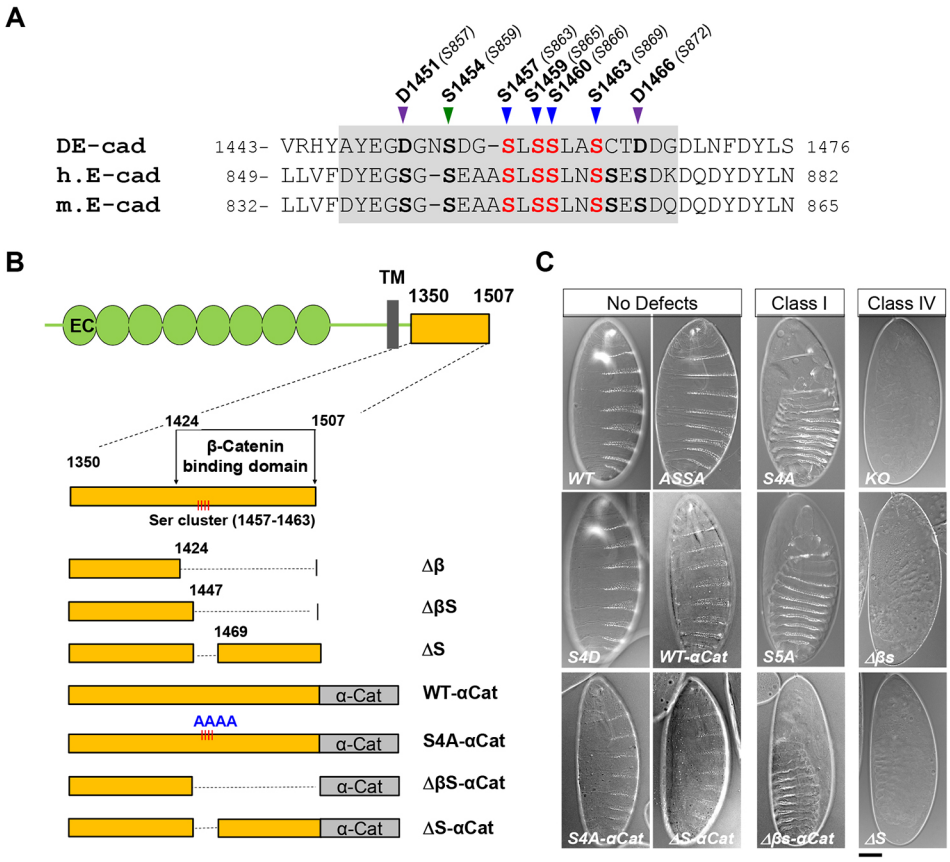

Fig. 1. The conserved serine cluster in DE-Cadherin is required for AJ formation and development. (A) Sequence alignment of the phospho-serine clusters from *Drosophila* (accession number: GI 17136470), human (GI 6682963) and mouse (GI 6753374) E-Cadherin intracellular domains. Shadowed box highlights the S-motif. Equivalent phospho-serines in human E-Cadherins are numbered in parentheses (Pacquelet and Rorth, 2005). (B) Schematic of DE-Cad structure and deletion/α-Cat fusion knock-in mutants. EC, extracellular cadherin domain; TM, transmembrane domain. Yellow box represents intracellular tail; gray box represents α-Catenin. (C) Cuticles prepared from zygotic homozygous embryos of selected viable and lethal *DE-Cad* mutants. Phenotype classifications are according to Tepass et al. (1996): Class I mutants show partial loss of cuticle whereas Class IV mutants show complete loss of cuticle. WT, wild type. (D) Mitotic clones generated in *FRT-G13 DE-CadΔβS::GFP*/*FRT-G13 His2Av::mRFP* larval wing disc by heat shock. *DE-CadΔβS::GFP* clones are labeled by the absence of nuclear RFP marker (from *His2Av::mRFP*), whereas twin wild-type clones are identified by the loss of DE-CadΔβS::GFP. Mutant cells show no discernable AJs by either GFP or β-Catenin staining and DE-CadΔβS::GFP only form intracellular puncta. However, *DE-CadΔβS::GFP* mutant cells maintained apical-basal polarity as evidenced by normal staining pattern of Baz and aPKC. Scale bars: 50 µm (C); 5 µm (D).

DE-Cadherin required for recruiting β-Catenin to AJ *in vivo*, we generated three *DE-Cad* knock-in mutants carrying deletions of 83aa (*DE-CadΔβ*), 60aa (*DE-CadΔβS*) or an internal 22aa (*DE-CadΔS*) that remove the conserved serine cluster (Fig. 1A,B). Similar to *DE-Cad*^{null} (*shg*^{2}), all three mutants are embryonic lethal (Table S1) with a severe loss-of-cuticle phenotype (Fig. 1C) that indicates a strong disruption of epithelial polarity and integrity. In larval wing disc epithelia, mutant cells expressing DE-CadΔβS and DE-CadΔS fail to form discernable AJs, which are labeled by junctional β-Catenin staining, and instead show cytosolic GFP^{+} puncta devoid of β-Catenin (Fig. 1D; Fig. 2A; all *DE-Cad* mutants generated in this report are tagged with GFP at the C terminus). The mutant clones are also of small and rounded shapes characteristic of *DE-Cad*^{null} mutant clones (Tepass et al., 1996). Such phenotypes suggest a complete loss of β-Catenin binding to DE-CadΔβS and DE-CadΔS and are consistent with the requirement of β-Catenin binding for trafficking of E-Cadherin to the plasma membrane (Chen et al., 1999). Loss of β-Catenin recruitment by DE-CadΔS is not simply due to the shortening of the DE-Cad intracellular tail, as a *DE-CadΔS+LK* knock-in allele with ΔS deletion replaced with a generic 22 aa linker (Varnai et al., 2006) showed phenotypes identical to *DE-CadΔS* (Fig. 2A). For clarity, we will hereafter refer to this 22 aa motif as 'S-motif' (Fig. 1A).

The conserved serine residues are required for DE-Cad functions in development in a quantitive manner

To identify whether any of the conserved serines in the S-motif are specifically required for β-Catenin recruitment, AJ formation and development, we generated an array of DE-Cad phospho-mutants (Table S1; Fig. 1A), which will hereafter be referred to collectively

Development (2017) 144, 1242-1248 doi:10.1242/dev.141598

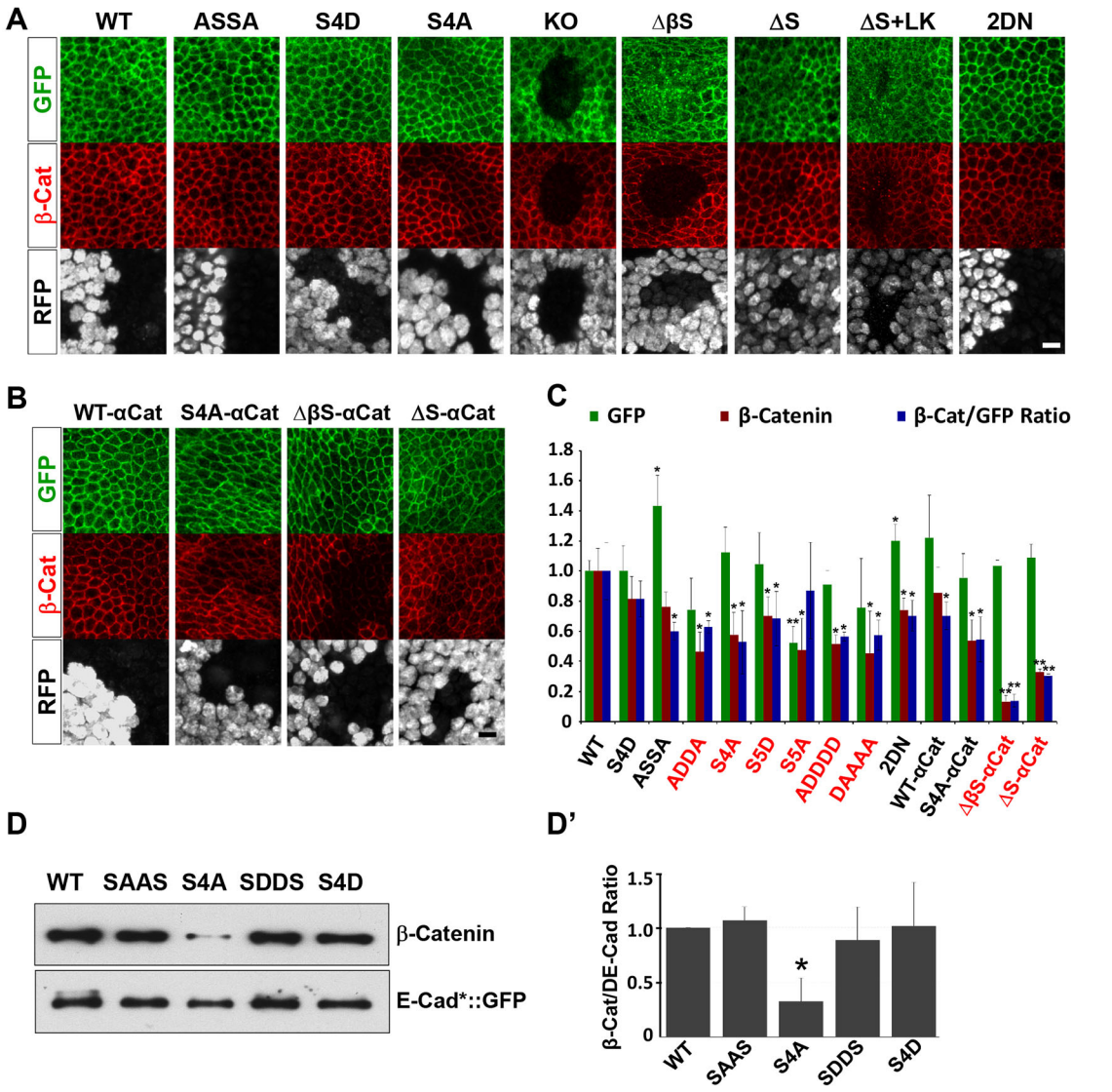

Fig. 2. Phosphorylation potential of the conserved serine cluster in the S-motif regulates AJ formation. (A,B) Immunostaining of larval wing disc epithelial clones of selected *DE-Cad* knock-in mutants. All mutant clones were generated against DE-Cad::GFP and are marked by loss of nuclear RFP. Wild-type twin clones are marked by increased RFP expression. (C) Measured GFP (i.e. DE-Cad*::GFP) and β-Catenin intensities and GFP/β-Catenin ratios in AJs in mutant clones. *DE-Cad*^{null} (i.e. *shg*^{2}) *DE-CadΔβS* and *DE-CadΔS* mutant cells do not form AJs and are therefore not are included. Names of lethal *DE-Cad** mutants are in red. (D) β-Catenin levels in AJ complexes immunoprecipitated from zygotic homozygous embryos of DE-Cad::GFP wild type or mutants as specified. (D′) Quantified β-Catenin/DE-Cad*::GFP ratios from the data shown in D, based on three separate rounds of immunoprecipitation results. *P<0.05, **P<0.005 (two-tailed *t*-test). KO, knockout; WT, wild type. Scale bar: 5 µm (for A and B).

as *DE-Cad**. Most of the *DE-Cad** mutants carried various combinations of single or multiple non-phosphorylatable S→A and/or phosphomimetic S→D mutations within the ^{1457}SLSSLAS serine cluster, which is nearly 100% conserved among the S-motifs of *Drosophila* and mammalian E-Cadherins (Fig. 1A). Viability tests (Table S1) suggest that *DE-Cad** mutants remain viable as long as two or more serine residues remain in the cluster. In addition, none of the four serine residues appears to be specifically required *in vivo* for DE-Cad functions in development (Table S1). Furthermore, *DE-CadS4D*, in which all four serine residues are mutated to phosphomimetic Asp, is homozygous viable, suggesting that regulating the phosphorylation of the SLSSLAS cluster is not essential for development. Our data are consistent with a model in which the overall phosphorylation level, rather than phosphorylation of any specific serine residues in S-motif, is crucial for DE-Cad function *in vivo*.

A recent study showed that phosphorylation of a conserved serine residue upstream of the SLSSLAS cluster directly regulates the stability of vertebrate E-Cadherin (McEwen et al., 2014). We thus generated mutants targeting ^{1454}Ser, which is the equivalent residue in DE-Cad (Fig. 1A). *DE-Cad* knock-in mutants carrying a single mutation of ^{1454}Ser→Ala or Asp (i.e. '*A-SSSS*' or '*D-SSSS*'; Table S1) are viable but such mutations are lethal when combined with S4D mutations (i.e. '*A-DDDD*' or '*D-DDDD*'; Table S1), suggesting that it is only in S4D mutants that the potential phosphorylation of ^{1454}Ser becomes essential for generating sufficient negative charges on the S-motif for recruiting β-Catenin (see below). Overall, in contrast to the results in cultured cells and in *C. elegans*, our data suggest that none of the conserved phospho-serines is specifically required for essential DE-Cad functions *in vivo*; instead, these serine residues appear to be required in a quantitative manner for viability and development.

Development (2017) 144, 1242-1248 doi:10.1242/dev.141598

Loss of phosphorylation potential of S-motif moderately reduces β-Catenin levels in AJs *in vivo*

We further focused on a subset of *DE-Cad** mutants to investigate how phospho-mutations in the S-motif affect AJ formation and β-Catenin/DE-Cad interactions *in vivo*. We used FRT-mediated mitotic recombination to generate simultaneously mitotic clones of both wild-type *DE-Cad::GFP* and mutant *DE-Cad*::GFP* in wing disc epithelia. As both wild-type and mutant DE-Cad proteins are tagged with GFP, their levels can be quantified in the same sample by immunostaining with an anti-GFP antibody, and co-immunostaining with an anti-β-Catenin antibody can be used to quantify β-Catenin levels simultaneously. In contrast to mutant clones of *DE-CadΔβS*, *ΔS* and *ΔS+LK* that show complete loss of AJs in larval disc epithelia, clones of all the examined *DE-Cad** phospho-mutants form apparently normal AJs in larval wing disc epithelia as judged by GFP and β-Catenin staining (Fig. 2A). Moreover, although *in vitro* studies showed that phosphorylation of the serine cluster on the S-motif increases β-Catenin binding to the E-Cadherin intracellular tail by several hundred fold (Huber and Weis, 2001), none of the AJs formed by DE-Cad* phospho-mutants shows more than 60% reduction of β-Catenin (Fig. 2A,C; Table S1). Even in AJs formed by non-phosphorylatable DE-CadS4A or DE-CadS5A, β-Catenin levels are only reduced to ∼56% and ∼46% of wild-type AJs, respectively (Fig. 2A,C). In AJ complex immunoprecipitated from zygotic *DE-CadS4A* mutant embryos, β-Catenin is also only reduced approximately three-fold (Fig. 2D,D′).

Why do AJs formed by non-phosphorylatable DE-Cad mutants such as S4A and S5A still contain high levels of β-Catenin? We noticed that the S-motif is also rich in acidic residues such as Asp and Glu (Fig. 1A). In particular, ^{1451}Asp and ^{1466}Asp residues in DE-Cad are in the same locations as ^{857}Ser and ^{872}Ser in human E-Cad and therefore might play phosphomimetic functions. We mutated both to Asn in the *DE-Cad2DN* mutant and found that the β-Catenin level is also reduced in AJs (Table S1). Taken together, our data suggest that the *in vivo* recruitment of β-Catenin to AJs depends on the total negative charges on the DE-Cad S-motif, including basal charges from acidic Asp and Glu residues and additional charges from phosphorylation of the conserved serine cluster.

Covalently linking α-Catenin to DE-Cad compensates for the loss of phosphorylation-dependent β-Catenin in AJ formation and development

Although removing potential phosphorylation on the S-motif only moderately reduces β-Catenin in AJs, *DE-Cad** mutants that reduce the β-Catenin levels by more than 30% in mutant AJs are consistently lethal (Fig. 2C; Table S1). Live imaging showed that *DE-CadS4A* maternal mutant embryos develop normally until germband retraction after which the epidermis appears to break down during dorsal closure (Movies 1 and 2), suggesting that AJs formed by DE-CadS4A might not be robust enough to support tissue remodeling in late embryogenesis. A major function of β-Catenin is to recruit α-Catenin, which attaches the AJ complex to F-actin by a tension-dependent mechanism (Buckley et al., 2014), and covalently linking α-Catenin to E-Cadherin can at least partially compensate for the loss of β-Catenin in AJ formation (Bianchini et al., 2015; Desai et al., 2013; Nagafuchi et al., 1994; Pacquelet et al., 2003; Sarpal et al., 2012). Indeed, fusion of α-Catenin completely rescues the developmental lethality of DE-CadS4A (Fig. 2B,C). Importantly, the rescue is not due to DE-CadS4A-αCat recruiting more β-Catenin, as AJs formed by DE-CadS4A-αCat show no obvious increase of β-Catenin compared with AJs of DE-CadS4A. Fusion of α-Catenin also rescued the AJ formation defects of DE-CadΔβS and DE-CadΔS, but both fusion mutants remain lethal (Table S1) with a very low level of β-Catenin recruited to AJs (Fig. 1B; Fig. 2B,C). Our data suggest that the major *in vivo* function of phosphorylation-dependent recruitment of β-Catenin by DE-Cad could be limited to enhancing the interaction between DE-Cad and α-Catenin, as loss of such β-Catenin can be fully compensated for by fusion of α-Catenin to DE-Cad for AJ formation and development. However, phosphorylation-independent recruitment of β-Catenin by DE-Cad has an essential role in development and cannot be compensated for by covalent fusion of α-Catenin to DE-Cad.

Conserved serine residues regulate the biosynthetic turnover of DE-Cad during apical-basal polarization

To investigate whether phosphorylation of the S-motif could regulate AJ turnover dynamics, we carried out whole-cell fluorescence recovery after photobleaching (FRAP) assays (Huang et al., 2011) to measure specifically the biosynthetic turnover rates of selected DE-Cad* mutants in polarizing and polarized cells (Fig. 3A; Fig. S1A,B; Table S1). Stage 9-11 embryos were selected for assaying polarizing epithelial cells and stage 15 embryos for assaying polarized cells. Whole-cell FRAP assays were performed in lateral epidermis (Huang et al., 2011). Although all DE-Cad* show reduced levels of β-Catenin in AJs *in vivo*, overall it appears that loss of phosphorylation potential of the SLSSLAS motif in DE-Cad does not significantly increase the biosynthetic instability of DE-Cad in AJs (Fig. 3A; Table S1). In contrast, fusion of α-Catenin to DE-CadS4A dramatically reduced DE-CadS4A turnover by 80%, making DE-CadS4A-αCat the most biosynthetically stable mutants we have characterized so far (Fig. 3A). This stabilizing effect is not due to α-Cat fusion to DE-Cad alone, as wild-type DE-Cad-αCat only showed mildly reduced biosynthetic turnover in polarizing cells (Fig. 3A). In addition, DE-CadASSA has significantly reduced biosynthetic turnover in polarizing cells and increased turnover in polarized cells – essentially a reversed differential regulation pattern of AJ dynamics compared with wild-type DE-Cad during cell polarization (Huang et al., 2011). Consistent with our whole-cell FRAP results, latrunculin treatment also showed that in *DE-CadS4A-αCat* and *DE-CadASSA* embryos the AJ-localized DE-Cad, and presumably AJs, are more resistant to the loss of F-actin (Fig. 3B). The viability of *DE-CadASSA* and *DE-CadS4A-αCat* mutants demonstrates that *Drosophila* can tolerate a surprisingly wide range of DE-Cad biosynthetic turnover rates during cell polarization and development.

Biosynthetically stable DE-Cad mutants rescue the polarity defects in *sdt* and *crb* embryonic epithelial cells

Sdt and Crb form an apical polarity complex that is essential for establishing apical-basal polarity in early embryonic epithelial cells, and their mutant embryos show identical defects in AJs and apical-basal polarity (Bachmann et al., 2001; Hong et al., 2001; Tepass and Knust, 1993). It has been proposed that the Sdt-Crb complex is specifically required in polarizing or remodeling cells subject to fast turnover of AJs (Campbell et al., 2009). To test this hypothesis directly, we combined *sdt* or *crb* with biosynthetically stable *DE-CadASSA* or *DE-CadS4A-αCat* mutants. In *DE-Cad; crb* and *DE-Cad::αCat; crb* mutant embryos, DE-Cad and DE-Cad::αCat, as well as the apical polarity marker Baz are all severely disrupted at early stages (Fig. 3C). In contrast, mutant embryos of *DE-CadASSA; crb*, or *sdt; DE-CadASSA* or *sdt; DE-CadS4A-αCat*

Development (2017) 144, 1242-1248 doi:10.1242/dev.141598

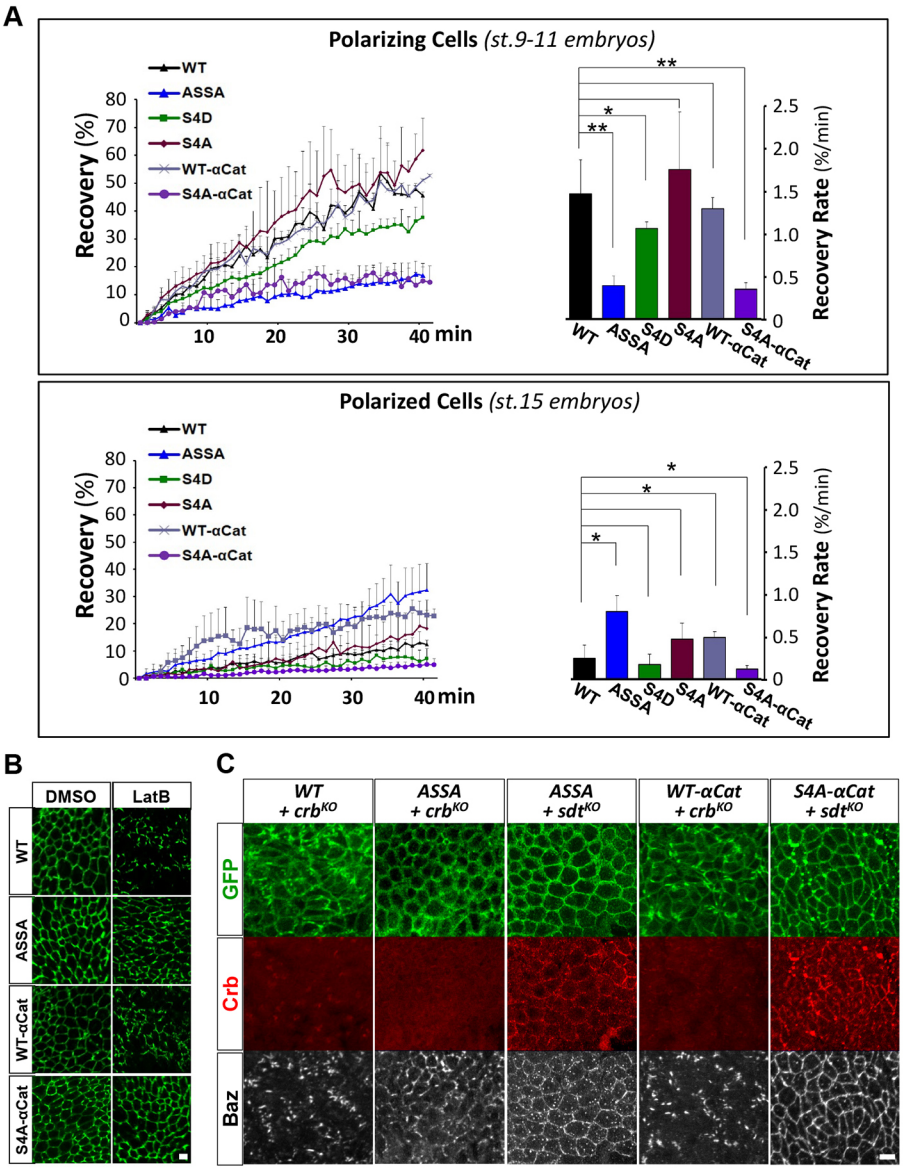

Fig. 3. Phospho-serines regulate the biosynthetic stability of DE-Cad in AJs. (A) Whole-cell FRAP results of selected DE-Cad* mutants in polarizing and polarized embryonic epithelial cells. *P<0.05, **P<0.005 (two-tailed t-test). (B) In early embryonic epithelia (stage 9-11), latrunculin (LatB) treatment severely disrupts the zonular AJs formed by wild-type (WT) DE-Cad::GFP and DE-Cad-αCat::GFP. AJs formed by DE-CadASSA and DE-CAdS4A-αCat are much more resistant. (C) Rescue of AJ and polarity defects in crb^{KO} and sdt^{KO} mutant embryonic epithelial cells by DE-CadASSA ('ASSA') and DE-CadS4A-αCat ('S4A-α-Cat'). WT: DE-Cad::GFP; WT-α-Cat: DE-Cad::α-Catenin::GFP. Embryos were between stages 11 and 12 of embryogenesis. Images were captured at lateral epidermis. Scale bars: 5 µm.

showed a dramatic rescue of AJ formation and polarity by restoring the apical localization of mutant DE-Cad and Baz (Fig. 3C). In addition, although Sdt and Crb are mutually dependent on each other for localizing to apical membrane (Hong et al., 2001), Crb apical localization was restored in mutant embryos of *sdt; DE-CadASSA* and *sdt; DE-CadS4A-αCat*. As expected, the more stable DE-CadS4A-αCat yielded a much stronger rescue of AJ formation and polarity defects than DE-CadASSA (Fig. 3C). Our data support the hypothesis that the Sdt-Crb complex is specifically required in polarizing cells undergoing fast AJ turnover, whereas in polarized cells biosynthetically stable AJs make Sdt-Cbr dispensable. Interestingly, *DE-CadASSA* or *DE-CadS4A-αCat* did not rescue Baz localization in amnioserosa cells in crb^{KO} or sdt^{KO} mutant embryos (data not shown), suggesting that the Sdt-Crb complex acts through mechanisms independent of AJ stability to maintain polarity in these actively constricting cells (David et al., 2010; Flores-Benitez and Knust, 2015; Harden et al., 2002).

In summary, we have shown that the conserved serine cluster motif is structurally required for AJ formation *in vivo*. Although a lack of proper antibodies meant that it was not possible for us to determine the phosphorylation levels of the serine cluster in wild-type and mutant DE-Cad proteins, the extremely conserved nature of the S-motif and the phenotypes of *DE-Cad* phospho-mutants support the suggestion that phosphorylation of the S-motif in DE-Cad is highly likely *in vivo*. However, our *in vivo* data showed that there is a surprisingly strong phosphorylation-independent recruitment of β-Catenin by DE-Cad that appears to be sufficient for AJ formation. Although phosphorylation-dependent recruitment of β-Catenin in AJs is indeed required for development, its role appears to be limited to enhancing the interaction between α-Catenin and the DE-Cad/β-Catenin complex. In contrast to transgenic rescue assays that showed that the ^{1457}Ser-equivalent residue in worm E-Cadherin is essential for development, our *Drosophila* knock-in mutants showed that none of the conserved serine residues is specifically required for AJ formation and development *in vivo*. Mechanisms reconciling such differences remain unclear to us, but our data are consistent with a model in which total negative charges on the conserved serine cluster enhance the potential binding between *Drosophila* DE-Cad and β-Catenin in AJs. However, site-specific phosphorylation of the serine cluster can dramatically regulate the biosynthetic stability of DE-Cad proteins in AJs, and it will be of great interest to identify

Development (2017) 144, 1242-1248 doi:10.1242/dev.141598

the specific serine residues and kinases that are involved in such regulation.

MATERIALS AND METHODS

Fly genetics

Generation of DE-Cad knock-in alleles was carried out by genomic engineering as described previously (Huang et al., 2009). DE-Cad mutants were recombined with *FRT-G13* chromosome for clonal analysis. Mutants of $crb^{[KO]}$ and $sdt^{[KO]}$ were described previously (Huang et al., 2009). Additional materials and methods For details of generation of larval mitotic recombinant clones and germline clones, and a full list of fly stocks and genotypes of samples presented in figure panels, see supplementary Materials and Methods.

Immunostaining and quantification

Immunostaining of wing discs and embryos were described previously (Huang et al., 2009). For primary and secondary antibodies, see supplementary Materials and Methods. Images were collected on Olympus FV1000 confocal microscopes (Center for Biologic Imaging, University of Pittsburgh Medical School, PA, USA) and processed in Adobe Photoshop for compositions. The images containing *z*-sections were analyzed using ImageJ and custom scripts in Photoshop. Junctional signals of GFP and β-Catenin were quantified using custom software as previously described (Huang et al., 2009).

Whole-cell FRAP assays and live imaging of embryogenesis

Staged embryos were collected and their eggshells were manually removed. Dechorionated embryos were placed in air-permeable chambers filled with halocarbon oil (#95) on custom-made slides, to ensure their normal development throughout the imaging session (Huang et al., 2011). Whole-cell FRAP assays were carried out using a Nikon confocal microscope A1 (Center for Biologic Imaging, University of Pittsburgh, PA, USA). Quantification of the FRAP recording images and data processing were described previously (Huang et al., 2011).

Cuticle preparation

Dechorionated embryos were mounted on slides in a mixture of lactic acid (S25374, Fisher Science Education) and Hoyer's solution (1:1). The slides were baked at 65°C for 16 h before imaging. Lethal DE-Cad mutants were balanced on CyO, twi-GFP chromosome and zygotic mutant embryos were identified by the absence of GFP expression prior to cuticle preparation.

Immunoprecipitation of DE-Cad/β-Catenin complex from embryos

Embryos were collected for 2 h at 25°C then aged for 4 h at 25°C for collecting early embryos or 10 h at 25°C for late embryos. Immunoprecipitation of the AJ complex and western blotting were carried out as previously described (Huang et al., 2009).

Drug treatments in embryos

Embryos were dechorionated in bleach, washed and then placed in a 1:1 mixture of Schneider's medium and *n*-octane (Teodoro and O'Farrell, 2003). Latrunculin (stock solution of 1 mM in DMSO; final concentration of 20 µM; Sigma, L5288) or an equal amount of DMSO were added to Schneider's medium and embryos were shaken at 400 rpm (on an orbital shaker) for 30 min. Embryos were then quickly rinsed in *n*-octane, briefly dried in air and immediately mounted in halocarbon oil (#95) in an air-permeable chamber for imaging.

Acknowledgements

We are grateful to Drs Fabrice Roegiers and Daniel Kiehart for reagents and fly stocks; Dr Simon Watkins and University of Pittsburgh Medical School Center for Biologic Imaging for generous imaging and microscopy support; Bloomington Stock Center for fly stocks; and Developmental Studies Hybridoma Bank (DSHB) for antibodies.

Competing interests

The authors declare no competing or financial interests.

Author contributions

Conceptualization: Y.H., Y.-J.C., J.H.; Investigation: Y.-J.C., J.H., L.H., E.A.; Writing – review and editing: Y.H., Y.-J.C.; Funding acquisition: Y.H.; Supervision: Y.H.

Funding

This work was supported by grants from the National Institutes of Health National Center for Research Resources [R21RR024869 to Y.H.] and the National Institutes of Health National Institute of General Medical Sciences [R01GM086423 to Y.H.]. The University of Pittsburgh Medical School Center for Biologic Imaging is supported by a grant from the National Institutes of Health [1S10OD019973-01]. Deposited in PMC for release after 12 months.

Supplementary information

Supplementary information available online at
http://dev.biologists.org/lookup/doi/10.1242/dev.141598.supplemental

References

Bachmann, A., Schneider, M., Theilenberg, E., Grawe, F. and Knust, E. (2001). Drosophila Stardust is a partner of Crumbs in the control of epithelial cell polarity. *Nature* **414**, 638-643.

Bianchini, J. M., Kitt, K. N., Gloerich, M., Pokutta, S., Weis, W. I. and Nelson, W. J. (2015). Reevaluating αE-catenin monomer and homodimer functions by characterizing E-cadherin/αE-catenin chimeras. *J. Cell Biol.* **210**, 1065-1074.

Buckley, C. D., Tan, J., Anderson, K. L., Hanein, D., Volkmann, N., Weis, W. I., Nelson, W. J. and Dunn, A. R. (2014). The minimal cadherin-catenin complex binds to actin filaments under force. *Science* **346**, 1254211.

Campbell, K., Knust, E. and Skaer, H. (2009). Crumbs stabilises epithelial polarity during tissue remodelling. *J. Cell Sci.* **122**, 2604-2612.

Chen, Y.-T., Stewart, D. B. and Nelson, W. J. (1999). Coupling assembly of the E-cadherin/beta-catenin complex to efficient endoplasmic reticulum exit and basal-lateral membrane targeting of E-cadherin in polarized MDCK cells. *J. Cell Biol.* **144**, 687-699.

Choi, H.-J., Huber, A. H. and Weis, W. I. (2006). Thermodynamics of beta-catenin-ligand interactions: the roles of the N- and C-terminal tails in modulating binding affinity. *J. Biol. Chem.* **281**, 1027-1038.

Choi, H.-J., Loveless, T., Lynch, A. M., Bang, I., Hardin, J. and Weis, W. I. (2015). A conserved phosphorylation switch controls the interaction between cadherin and β-catenin in vitro and in vivo. *Dev. Cell* **33**, 82-93.

David, D. J. V., Tishkina, A. and Harris, T. J. C. (2010). The PAR complex regulates pulsed actomyosin contractions during amnioserosa apical constriction in Drosophila. *Development* **137**, 1645-1655.

Desai, R., Sarpal, R., Ishiyama, N., Pellikka, M., Ikura, M. and Tepass, U. (2013). Monomeric α-catenin links cadherin to the actin cytoskeleton. *Nat. Cell Biol.* **15**, 261-273.

Flores-Benitez, D. and Knust, E. (2015). Crumbs is an essential regulator of cytoskeletal dynamics and cell-cell adhesion during dorsal closure in Drosophila. *Elife* **4**, e07398.

Harden, N., Ricos, M., Yee, K., Sanny, J., Langmann, C., Yu, H., Chia, W. and Lim, L. (2002). Drac1 and Crumbs participate in amnioserosa morphogenesis during dorsal closure in Drosophila. *J. Cell Sci.* **115**, 2119-2129.

Harris, T. J. C. and Tepass, U. (2010). Adherens junctions: from molecules to morphogenesis. *Nat. Rev. Mol. Cell Biol.* **11**, 502-514.

Hong, Y., Stronach, B., Perrimon, N., Jan, L. Y. and Jan, Y. N. (2001). Drosophila Stardust interacts with Crumbs to control polarity of epithelia but not neuroblasts. *Nature* **414**, 634-638.

Huang, J., Zhou, W., Dong, W., Watson, A. M. and Hong, Y. (2009). Directed, efficient, and versatile modifications of the Drosophila genome by genomic engineering. *Proc. Natl. Acad. Sci. USA* **106**, 8284-8289.

Huang, J., Huang, L., Chen, Y.-J., Austin, E., Devor, C. E., Roegiers, F. and Hong, Y. (2011). Differential regulation of adherens junction dynamics during apical-basal polarization. *J. Cell Sci.* **124**, 4001-4013.

Huber, A. H. and Weis, W. I. (2001). The structure of the β-catenin/E-cadherin complex and the molecular basis of diverse ligand recognition by β-catenin. *Cell* **105**, 391-402.

Lickert, H., Bauer, A., Kemler, R. and Stappert, J. (2000). Casein kinase II phosphorylation of E-cadherin Increases E-cadherin/β-catenin interaction and strengthens cell-cell adhesion. *J. Biol. Chem.* **275**, 5090-5095.

McEwen, A. E., Maher, M. T., Mo, R. and Gottardi, C. J. (2014). E-cadherin phosphorylation occurs during its biosynthesis to promote its cell surface stability and adhesion. *Mol. Biol. Cell* **25**, 2365-2374.

Nagafuchi, A., Ishihara, S. and Tsukita, S. (1994). The roles of catenins in the cadherin-mediated cell adhesion: functional analysis of E-cadherin-alpha catenin fusion molecules. *J. Cell Biol.* **127**, 235-245.

Oda, H., Uemura, T., Shiomi, K., Nagafuchi, A., Tsukita, S. and Takeichi, M. (1993). Identification of a Drosophila homologue of alpha-catenin and its association with the armadillo protein. *J. Cell Biol.* **121**, 1133-1140.

Pacquelet, A. and Rørth, P. (2005). Regulatory mechanisms required for DE-cadherin function in cell migration and other types of adhesion. *J. Cell Biol.* **170**, 803-812.

Development (2017) 144, 1242-1248 doi:10.1242/dev.141598

Pacquelet, A., Lin, L. and Rorth, P. (2003). Binding site for p120/delta-catenin is not required for Drosophila E-cadherin function in vivo. *J. Cell Biol.* **160**, 313-319.

Peifer, M. and Wleschaus, E. (1990). The segment polarity gene armadillo encodes a functionally modular protein that is the Drosophila homolog of human plakoglobin. *Cell* **63**, 1167-1178.

Sarpal, R., Pellikka, M., Patel, R. R., Hui, F. Y. W., Godt, D. and Tepass, U. (2012). Mutational analysis supports a core role for Drosophila α-Catenin in adherens junction function. *J. Cell Sci.* **125**, 233-245.

Stappert, J. and Kemler, R. (1994). A short core region of E-cadherin is essential for catenin binding and is highly phosphorylated. *Cell Adhes. Commun.* **2**, 319-327.

Tepass, U. and Knust, E. (1993). Crumbs and stardust act in a genetic pathway that controls the organization of epithelia in Drosophila melanogaster. *Dev. Biol.* **159**, 311-326.

Tepass, U., Gruszynski-DeFeo, E., Haag, T. A., Omatyar, L., Torok, T. and Hartenstein, V. (1996). shotgun encodes Drosophila E-cadherin and is preferentially required during cell rearrangement in the neurectoderm and other morphogenetically active epithelia. *Genes Dev.* **10**, 672-685.

Teodoro, R. O. and O'Farrell, P. H. (2003). Nitric oxide-induced suspended animation promotes survival during hypoxia. *EMBO J.* **22**, 580-587.

Varnai, P., Thyagarajan, B., Rohacs, T. and Balla, T. (2006). Rapidly inducible changes in phosphatidylinositol 4,5-bisphosphate levels influence multiple regulatory functions of the lipid in intact living cells. *J. Cell Biol.* **175**, 377-382.

SUPPLEMENTARY MATERIALS AND METHODS:

Fly Stocks: In addition to knock-in alleles listed in Table 1, the following stocks were used: *w; His2Av::mRFP ("Histone::RFP", BL#23651); hs-FLP* w^{1118}*;* adv^{1}*/CyO* (BL#6); *hs-FLP* w^{1118}*; FRT-G13 His2Av::mRFP DE-Cad::GFP*; *ovo-FLP w (BL#8727); FRT-G13* $ovoD^{1\text{-}18}$*/Dp(?;2)*bw^{D} S^{1} $wg^{Sp\text{-}1}$ *Ms(2)*M^{1} bw^{D}*/CyO* (BL#2125); y^{1} *w* N^{1}*/FM7c, twi-Gal4 UAS-2xGFP ("twi-GFP"* on X chromosome, BL#6873); w^{1118}*; In(2LR)Gla,* $wg^{Gla\text{-}1}$*/Cyo, twi-Gal4 UAS-2xGFP ("twi-GFP"* on 2nd chromosome, BL#6662); w^{1118}*;* Dr^{Mio}*/TM3, twi-Gal4 UAS-2xGFP ("twi-GFP"* on 3rd chromosome, BL#6663); cn^{1} shg^{2} bw^{1} sp^{1}*/CyO* (BL#3085); *y w* sdt^{XP1} *FRT-9-2/FM7c* (Hong et al., 2001); *y w;* crb^{11e22} */ TM3 Sb e* (gift from Dr. Knust (Klebes and Knust, 2000)).

Generation of larval mitotic recombinant clones and germline clones: For generating larval disc clones, virgin females of *hs-FLP w; FRT-G13 His2Av::RFP DE-Cad::GFP* were crossed with males of *y w/Y; FRT-G13 DE-Cad**. Parental flies were transferred every two days under 25 °C. At 72 and 96 hours after egg laying vials containing the first and second instar larvae after the transfer were heat-shocked in a 37°C water bath for 1.5 hours per day. Five to six days after egg laying heat-shocked third instar larvae were dissected for wing discs which were fixed for 1 hour in 4% formaldehyde for immunostaining. Maternal and zygotic mutant embryos were generated by germline clones (GLC) according to the published protocol (Chou and Perrimon, 1996) except that *ovo-FLP* was used in lieu of *hs-FLP*.

Antibodies: Primary antibodies: chicken anti-GFP (Aves Lab, cat# GFP-1010) 1:5000; home-made rabbit anti-GFP (Huang et al., 2009) 1:1500; mouse anti-RFP (Thermo Fisher Scientific, MA5-15257) 1:500; mouse anti-β-catenin (DSHB, N2 7A1) 1:100; guinea pig anti-Baz (Huang et al., 2009); mouse anti-Crb (DSHB, cq4-c) 1:10; rabbit anti-aPKC (Santa Cruz, Sc-216) 1:1000. Secondary antibodies: Cy2- , Cy3 or Cy5-conjugated goat anti-rabbit IgG, anti-mouse IgG, and anti-guinea pig IgG (The Jackson ImmunoResearch Lab, 111-225-003, 115-165-003, and 106-175-003), all at 1:400.

REFERENCES

Chou, T. B. and Perrimon, N. (1996). The autosomal FLP-DFS technique for generating germline mosaics in Drosophila melanogaster. *Genetics* **144**, 1673-1679.

Klebes, A. and Knust, E. (2000). A conserved motif in Crumbs is required for E-cadherin localisation and zonula adherens formation in Drosophila. *Curr. Biol.* **10**, 76-85.

Development • Supplementary information

Genotypes of *Drosophila* Samples Presented in Figures:

Figure 1C:

"WT": *w*^{1118};

"S4D": *y w; FRT-G13 DE-CadS4D::GFP;*

"S4A-αCat": *y w; FRT-G13 DE-CadS4A::α-Cat::GFP;*

"ASSA": *y w; FRT-G13 DE-CadASSA::GFP;*

"WT-αCat": *y w; FRT-G13 DE-Cad::α-Cat::GFP;*

"ΔS-αCat": *y w; FRT-G13 DE-CadΔS::α-Cat::GFP;*

"S4A": *y w; FRT-G13 DE-CadS4A::GFP;*

"S5A": *y w; FRT-G13 DE-CadS5A::GFP;*

"ΔβS-αCat": *y w; FRT-G13 DE-CadΔβS::α-Cat::GFP;*

"KO": *y w; FRT-G13 DE-Cad*^{KO}*::GFP;*

"ΔβS": *y w; FRT-G13 DE-CadΔβS::GFP;*

"ΔS": *y w; FRT-G13 DE-CadΔS::GFP;*

Figure 1D:

*hs-FLP w / y w (*or *Y); FRT-G13 DE-Cad*$^{\Delta\beta S}$*-α-Cat::GFP / FRT-G13 His2Av::RFP; +/+.*

Cross: hs-FLP w; FRT-G13 His2Av::RFP / CyO (X) y w / Y; FRT-G13 DE-CadΔβS::α-Cat::GFP / CyO twi-GFP (X)

Figure 2A:

"WT": *hs-FLP w / y w (*or *Y); FRT-G13 DE-Cad::GFP / FRT-G13 His2Av::RFP DE-Cad::GFP;*

"ASSA": *hs-FLP w / y w (*or *Y); FRT-G13 DE-CadASSA::GFP / FRT-G13 His2Av::RFP DE-Cad::GFP;*

"S4D": *hs-FLP w / y w (*or *Y); FRT-G13 DE-CadS4D::GFP / FRT-G13 His2Av::RFP DE-Cad::GFP;*

"S4A": *hs-FLP w / y w (*or *Y); FRT-G13 DE-CadS4A::GFP / FRT-G13 His2Av::RFP DE-Cad::GFP;*

"KO": *hs-FLP w / y w (*or *Y); FRT-G13 DE-Cad*^{KO}*::GFP/ FRT-G1 His2Av::RFP DE-Cad::GFP;*

"ΔβS": *hs-FLP w / y w (*or *Y); FRT-G13 DE-CadΔβS::GFP / FRT-G13 His2Av::RFP DE-Cad::GFP;*

"ΔS": *hs-FLP w / y w (*or *Y); FRT-G13 DE-CadΔS::GFP / FRT-G13 His2Av::RFP DE-Cad::GFP;*

"ΔβS+LK": *hs-FLP w / y w (*or *Y); FRT-G13 DE-CadΔβS+LK::α-Cat::GFP / FRT-G13 His2Av::RFP DE-Cad::GFP;*

"2DN": *hs-FLP w / y w (*or *Y); FRT-G13 DE-Cad2DN::GFP / FRT-G13 His2Av::RFP DE-Cad::GFP;*

Development • Supplementary information

Figure 2B:

"WT-αCat": *hs-FLP w / y w (*or *Y); FRT-G13 DE-Cad::α-Cat::GFP / FRT-G13 His2Av::RFP DE-Cad::GFP;*

"S4A-αCat": *hs-FLP w / y w (*or *Y); FRT-G13 DE-CadS4A::α-Cat::GFP / FRT-G13 His2Av::RFP DE-Cad::GFP;*

"ΔβS-αCat": *hs-FLP w / y w (*or *Y); FRT-G13 DE-CadΔβS::α-Cat::GFP / FRT-G13 His2Av::RFP DE-Cad::GFP;*

"ΔS-αCat": *hs-FLP w / y w (*or *Y); FRT-G13 DE-CadΔS::α-Cat::GFP / FRT-G13 His2Av::RFP DE-Cad::GFP;*

Figure 2D: embryos were collected from the following stocks:

"WT": *y w; FRT-G13 DE-Cad::GFP*

"ASSA": *y w; FRT-G13 DE-CadASSA::GFP*

"S4A": *y w; FRT-G13 DE-CadS4A::GFP / CyO;*

"SDDS": *y w; FRT-G13 DE-CadSDDS::GFP*

"S4D": *y w; FRT-G13 DE-CadS4A::GFP*

Figure 3A and Figure S1A,B:

"WT": w^{1118};

"ASSA": *y w; FRT-G13 DE-CadASSA::GFP ;*

"S4D": *y w; FRT-G13 DE-CadS4D::GFP ;*

"S4A": *y w; FRT-G13 DE-CadS4A::GFP*^{GLC} *;(maternal and zygotic mutant embryo)*

"WT-αCat": *y w; FRT-G13 DE-Cad::α-Cat::GFP ;*

"S4A-αCat": *y w; FRT-G13 DE-CadS4A::α-Cat::GFP ;*

Figure 3B:

"WT": w^{1118};

"ASSA": *y w; FRT-G13 DE-CadASSA::GFP ;*

"WT-αCat": *y w; FRT-G13 DE-Cad::α-Cat::GFP ;*

"S4A-αCat": *y w; FRT-G13 DE-CadS4A::α-Cat::GFP ;*

Figure 3C:

"*WT* + *crb*^{KO}": (stage 12 embryo)

y w; FRT-G13 DE-Cad::GFP; crb^{KO}

Stock: y w; FRT-G13 DE-Cad::GFP; crb^{KO}*/TM3 twi-GFP*

Development • Supplementary information

"*ASSA + crb^{KO}*": (stage 10 embryo)

y w; FRT-G13 DE-CadASSA::GFP; crb^{KO}

Stock: y w; FRT-G13 DE-CadASSA::GFP; crb^{KO}/TM3 twi-GFP

"*ASSA + sdt^{KO}*": (stage 11 embryo)

w sdt^{KO}/ Y; FRT-G13 DE-CadASSA::GFP

Stock: w sdt^{KO}/FM7c twi-GFP; DE-CadASSA::GFP

"*WT-αCat + crb^{KO}*": (late stage 11 embryo)

y w; FRT-G13 DE-Cad-α-Cat::GFP; crb^{KO}

Stock: y w; FRT-G13 DE-Cad-α-Cat::GFP; crb^{KO} / TM3 twi-GFP

"*S4A-αCat + sdt^{KO}*": (late stage 11 embryo)

w sdt^{KO}/ Y; FRT-G13 DE-CadS4A::α-Cat::GFP ;

Stock: w sdt^{KO} / FM7c twi-GFP; DE-Cad S4A-αCat::GFP

Development • Supplementary information

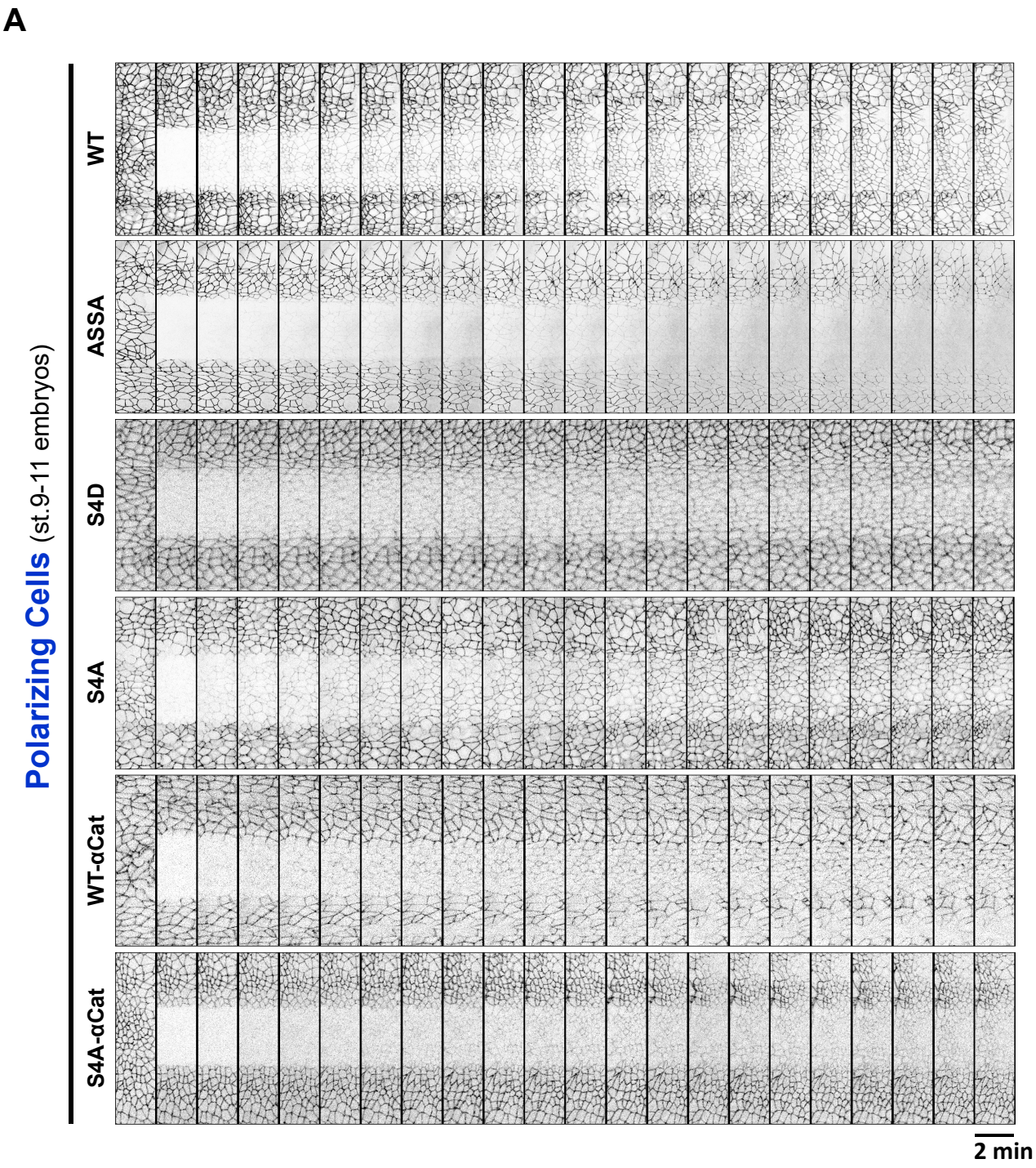

Development • Supplementary information

B

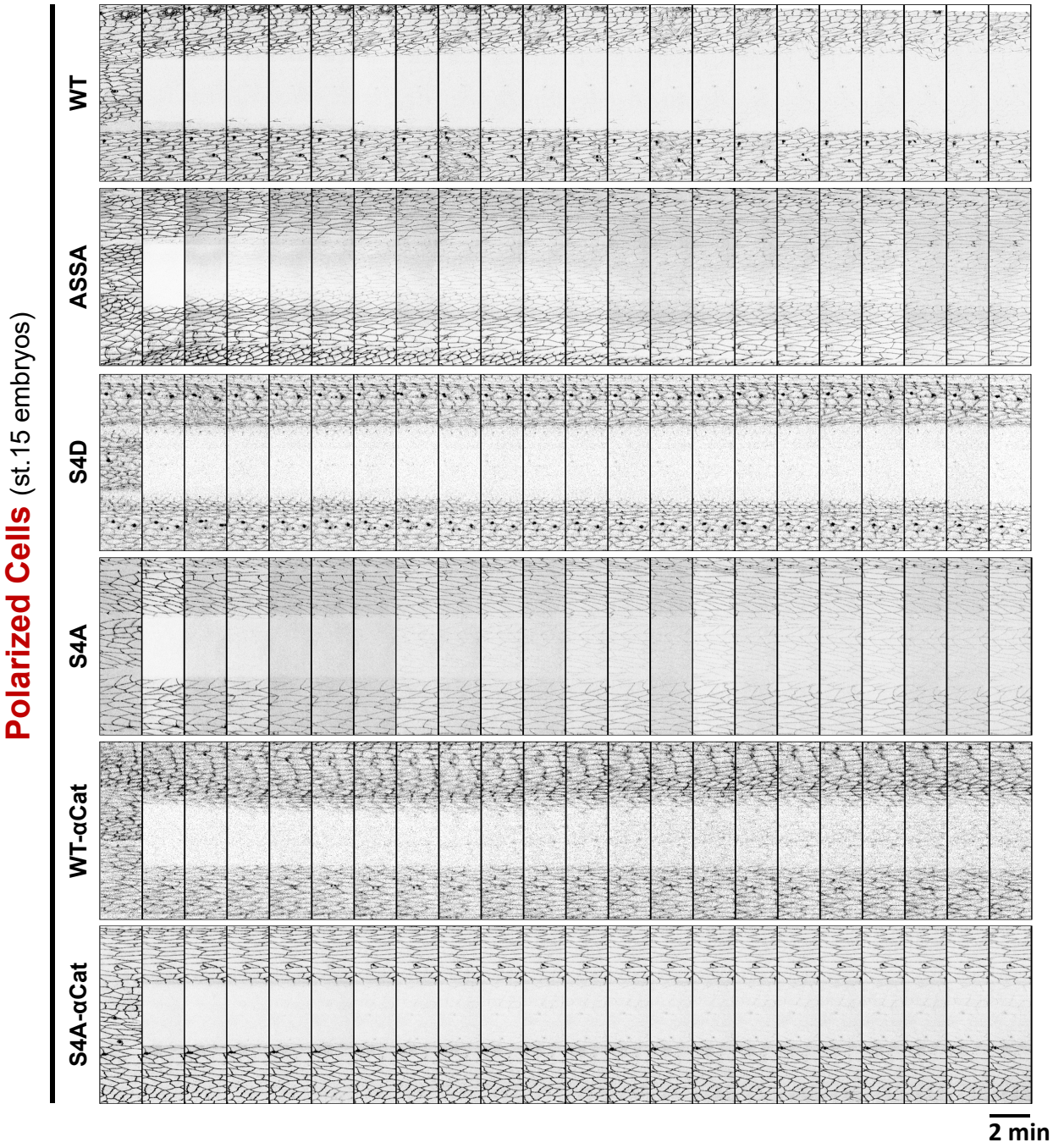

Figure S1. Biosynthetic turnover of DE-Cad* mutants in embryonic epithelia measured by whole-cell FRAP assays.

(**A-B**) Representative whole-cell FRAP samples of selected DE-Cad* mutants in stage 9-11 early embryos (A, for measuring in polarizing embryonic epithelial cells) and stage 15 late embryos (B, for measuring in polarized embryonic epithelial cells). In each whole-cell FRAP sample, GFP in a patch of lateral embryonic epithelium was completely bleached therefore the GFP can only recover from de novo synthesis of DE-Cad. For presentation purpose images were processed in Photoshop to achieve enhanced contrast. All quantifications were done in original unadjusted images.

Development • Supplementary information

Table S1. DE-Cad knock-in mutants. All *DE-Cad* knock-in mutants are tagged with GFP at the C-terminus. Point mutations of phospho-serines in each allele are marked in an "S-SSSS" format abbreviating for Ser-1454, 1457, 1459, 1460 and 1463 in DE-Cad (see Fig. 1A). Each lethal allele was also confirmed by their lethality over the *shg*^{2} null allele, to exclude the possibility of background lethal mutations. Lethal phase of each allele was determined in zygotic homozygotes. DE-Cad*::GFP and β-Catenin levels in mutant AJs were normalized against measurements in AJs formed by wild type DE-Cad::GFP in neighboring twin clones. In parentheses are the numbers of FRAP assays (one assay per embryo, 3rd and 4th columns) or clones quantitatively measured in immunostaining assays (the last three columns). Due to slow recovery of many whole-cell FRAP samples it is impractical to record FRAP long enough to calculate the $t_{1/2}$ and mobile/immobile fractions, therefore we calculated recovery rates as %/min linear rate based on the recovery within the first five to ten minutes (Huang et al., 2011). V: viable. "\": not done. Quantitative data are presented as mean±s.d.

Click here to Download Table S1

Development • Supplementary information

SUPPLEMENTARY MOVIES

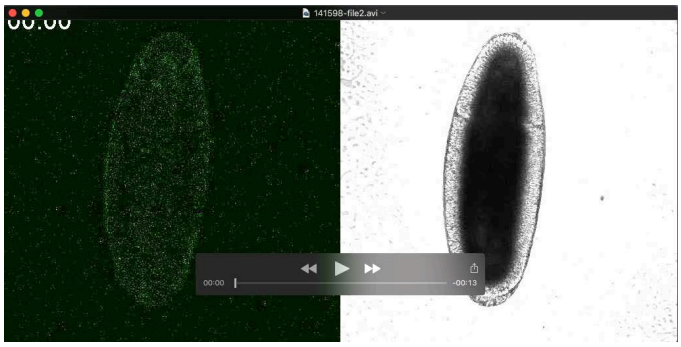

Movie 1. Embryogenesis of maternal mutant embryo of *DE-CadS4A::GFP*. The movie is recorded by time-laps from starting stage 7 at 5min interval. The total recording time is 9 hours, with GFP channel at left and DIC channel at right. The genotype the embryo (*ovo-FLP w / +; FRT-G13 DE-CadS4A::GFP*) was confirmed by the absence of *twi-Gal4 UAS-GFP* expression. DE-CadS4A::GFP is too weak to be seen in this recording. Note the failed germ-band retraction starting 06:30 in DIC channel. Time stamp in “hh:mm” format.

Development • Supplementary information

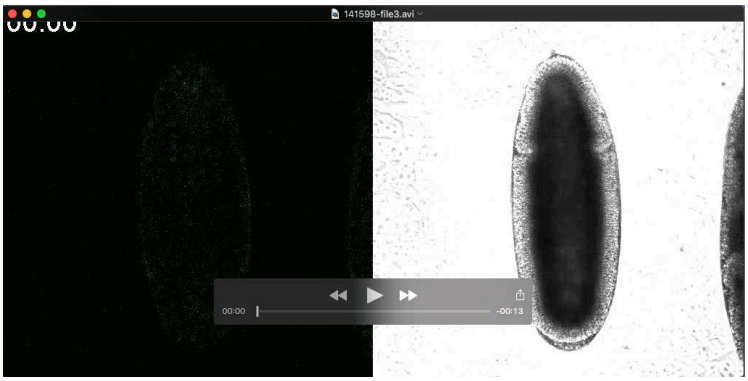

Movie 2. Embryogenesis of zygotically rescued maternal mutant embryo of *DE-CadS4A::GFP*. The sample embryo was recorded simultaneously with the embryo in Movie S1. Wild type genotype (*ovo-FLP w / +; FRT-G13 DE-CadS4A::GFP / CyO twi-GFP*) was confirmed by *twi-GFP* expression starting 06:00. Time stamp in “hh:mm” format.

Development • Supplementary information